Environmental modelling in the Gulf of Cadiz: Heavy metal distributions in water and sediments

R. Periáñez *

Dpto. Física Aplicada I, E.U. Ingeniería Técnica Agrícola, Universidad de Sevilla. Ctra. Utrera km 1, 41013-Sevilla, Spain

Keywords: Numerical modelling
Hydrodynamics
Sediment transport
Heavy metals
Gulf of Cadiz

A B S T R A C T

The Gulf of Cadiz (GoC) connects the Atlantic Ocean and the Mediterranean Sea. An environmental study of the GoC is carried out through numerical modelling. First, a 3D baroclinic model is used to obtain the residual circulation and a 2D barotropic model is applied to calculate tides. The results of these models are used by a 3D sediment transport model which provides suspended matter concentrations and sedimentation rates in the GoC. Then heavy metal dispersion patterns are investigated using a 3D model which includes water–sediment metal interactions and uses the outputs of the hydrodynamic and sediment transport models. The metal transport model has been applied to simulate the dispersion of Zn, Cu and Ni introduced into the GoC from three rivers draining the Iberian Pyrite Belt, in the southern Iberian Peninsula. Results from the hydrodynamic, sediment and metal transport models have been compared with measurements in the GoC. In particular, the contamination of sediments collected along the southern coast of Spain is well reproduced by the model. Metal plumes reach the Strait of Gibraltar, thus the three rivers constitute a source of pollutants into the Mediterranean Sea.

1. Introduction

The Gulf of Cadiz (GoC) is the sub-basin of the Atlantic Ocean which is nearest to the Strait Of Gibraltar, connecting the Atlantic Ocean and the Mediterranean Sea. Its northern, southern and eastern boundaries are, respectively, the Atlantic coasts of Spain, Morocco and the Strait of Gibraltar. The western boundary is usually defined by the 9°W meridian (Fig. 1).

Recently, the GoC has been the subject of oceanographic studies dealing with surface and deep circulation, aimed at understanding the mechanisms of water exchange between the Atlantic Ocean and the Mediterranean Sea; as well as the behaviour of the dense plume of Mediterranean water (Ambar and Howe, 1979; García-Lafuente et al., 2006; Criado-Aldeanueva et al., 2006; Machín et al., 2006; García-Lafuente and Ruíz, 2007). The distribution of suspended matter and sediment transport in the GoC has also been investigated (Gonzalez et al., 2007; Freitas and Abrantes, 2002; Lobo et al., 2004; Cravo et al., 2006; Palanques et al., 1986–1987).

The freshwater inputs of rivers discharging in the GoC are relatively small. However, the Guadalquivir, Guadiana and Odiel–Tinto rivers, in the southern Iberian Peninsula (Fig. 1), present strongly enhanced heavy metal concentrations since they drain the Iberian Pyrite Belt (Sainz and Ruiz, 2006), one of the most important mining areas in the south of Europe. Mineral resources have been extracted in the last 5000 years during two main periods: the Roman age and the last two centuries. During the last period, intensive exploitation has led to a relevant environmental impact, with vast surfaces covered with mining residues and subjected to erosion (Sainz and Ruiz, 2006). The GoC is responsible for 5–10% of fish and shell-fish catches of Spain and Portugal (Beckers et al., 2007), holding important living resources of commercial and ecological interest. Consequently, it is relevant to study and understand the geochemistry and dispersion patterns of heavy metals in the GoC system, since this will help assessing the potential influence of metals on ecosystem functioning. Thus, several papers concerning the distribution of metals in the GoC have been published in the last years (Sainz and Ruiz, 2006; Morillo et al., 2004; Elbaz-Poulichet et al., 2001; Fernández-Caliani et al., 1997). Indeed, studies on the distribution of trace metals in coastal waters are frequently published in recent times (see for instance Li et al., 2007; Suntornvongsagula et al., 2007; Cuong et al., 2008; Chen and Jiao, 2008; Valdés et al., 2008; Marín-Guirao et al., 2008).

The objective of this work consists of studying the dynamics of heavy metals in the northern GoC by means of numerical modelling. Models have been widely applied to simulate contaminant dispersion since they may provide insights on the main environmental processes governing such dispersion and, consequently, may help to describe and characterize the environment (Scott, 2003). In particular, models have been widely applied to heavy metal (Tappin et al., 1997; Wu et al., 2005; Prandle et al., 1996; Liu et al., 1998) and radioactive element (Harms, 1997; Cetina et al., 2000; Periáñez, 2003; Monte et al., 2006) dispersion in coastal waters.

* Fax: +34 954486436.
E-mail address: rperianez@us.es.

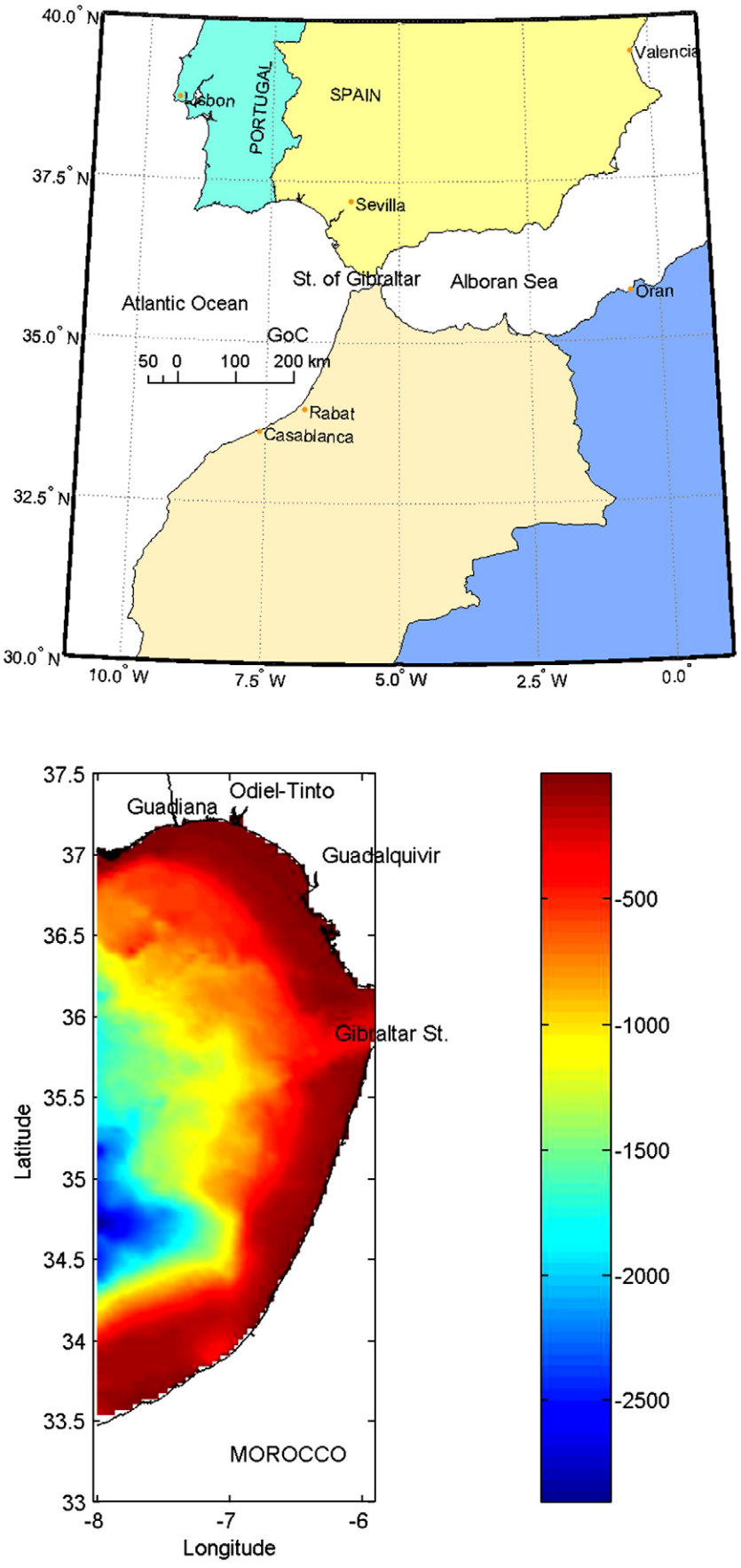

Fig. 1. General localization of the study area and topography of the GoC (depths in m). The localization of Guadiana, Odiel–Tinto and Guadalquivir rivers is also shown.

Although some interesting modelling works describing water circulation off Iberia and Morocco coasts have been published (Johnson and Stevens, 2000; Batteen et al., 2000), these models have a relatively low resolution, not providing detailed information about the GoC basin circulation features. In the first case, spatial resolution is 10 min in both longitude and latitude (5 times the grid cell in the present model). In the second reference it is 10 km in longitude and latitude, about three times larger than in this work. Other modelling works are specifically devoted to the study of Mediterranean water spreading (Jungclaus and Mellor, 2000; Johnson et al., 2002; Serra et al., 2005). The excellent paper by Peliz et al. (2007) presents three nested model domains aimed at reproducing known features of the Azores current and of circulation inside the GoC.

Published models describing trace metal dispersion in the GoC consider metals as conservative tracers, no interacting with sediments and without any other sources and sinks (Elbaz-Poulichet et al., 2001; Beckers et al., 2007). The first authors use a model to estimate the dilution of a conservative tracer released by the Odiel–Tinto rivers. Beckers et al. (2007) apply a numerical model to reproduce observed metal (again considering metals as conservative tracers) concentrations in surface waters of the northern GoC. Analysis of model results showed that sources/sinks of metals due to interactions with sediments (adsorption/desorption reactions as well as erosion and deposition processes) were apparent. Models which try to reproduce measured levels of metals in bed sediments of the GoC have not been published yet, to the author's knowledge.

The model described in this paper consists of three sub-models: firstly, a hydrodynamic module which provides currents over the domain. Two hydrodynamic models are used. A 2D barotropic model is applied to calculate tides and 3D baroclinic model is used to obtain the residual (mean) circulation. Tidal currents must be calculated since they may increase the bed stress and hence enhance sediment resuspension and affect deposition of particles as well. Indeed, the second sub-model is a sediment transport model which provides suspended matter concentrations and sedimentation rates over the domain. The third sub-model is the metal transport module, which includes advection/diffusion plus uptake/release reactions of metals between the dissolved and solid (suspended matter in the water column and bed sediments) phases.

The three modules, as well as the numerical techniques used to solve the involved equations are described in Section 2. Next, model results are discussed separately for water circulation, sediment transport and metal distributions. Some sensitivity analysis are finally described.

2. Model description

2.1. Hydrodynamic models

As commented above, tides are required to calculate bed stress over the domain, since it will affect sedimentation rates in the shallower areas and/or where stronger tidal currents exist. A 2D depth-averaged model has been applied to calculate surface tides. This is a reasonable approach that has already been successfully used in the Strait of Gibraltar (Tejedor et al., 1999; Periáñez and Pascual-Granged, 2008), the Alborán Sea (Periáñez, 2008) and even in the complete Mediterranean Sea (Tsimplis et al., 1995). As has been shown, it is safe to neglect density differences in tidal computations (Dyke, 2001; Yanagi, 1999).

Equations are standard and may be seen for instance in Periáñez (2005a). The solution of these equations provides the water currents at each point in the model domain and for each time step. Currents are treated through standard tidal analysis (Pugh, 1987) and tidal constants are stored in files that will be read by the sediment transport model. The barotropic model includes the two main tidal constituents, M_2 and S_2. Thus, the hydrodynamic equations are solved for each constituent and tidal analysis is also carried out for each constituent separately.

The long-term circulation is obtained from a full 3D, primitive equation, baroclinic hydrodynamic model. It is based upon the hydrostatic and Boussinesq approximations on a β plane. The model includes equations for salinity and temperature evolution and water density is calculated from them using a standard state equation (Batteen et al., 2000). The one-equation turbulence model described in Periáñez (2005b) has been used to calculate the vertical eddy viscosity. Details on the 3D equations may be seen, for instance, in Kowalick and Murty (1993). A summary of the main equations involved in both hydrodynamic models is presented in Appendix A.

2.2. Sediment transport

The transport of sediments is described by a 3D advection–diffusion equation to which some terms are added. These are external sources of particles (river supply), terms describing particle deposition on the seabed and erosion from the bed to the water column, and vertical settling. The formulation of these processes is based upon standard formulae. Thus, the erodability constant is used for the erosion term. Particle settling and deposition are described using the settling velocity, which is obtained from Stoke's law. Critical erosion and deposition stresses are used as usual. Details on the mathematical formulation may be seen elsewhere (Periáñez, 2005b; Liu et al., 2002a; Lumborg and Windelin, 2003; Cancino and Neves, 1999). Finally, it is also possible to calculate net sedimentation rates (SR) as the balance between the deposition and erosion terms. A summary of the equations may be seen in Appendix B.

2.3. Metal transport

Non conservative pollutants are those which do not remain dissolved in the water column, but have a certain affinity to be fixed to particles (suspended matter and bed sediments). Thus, three phases are included in the model: dissolved, suspended particles and bed sediments. Only fine sediments are considered (particles with diameter <62.5 μm) since metals are predominantly fixed to these (Eisma, 1993). The exchanges between the dissolved and solid phases may be described in terms of kinetic transfer coefficients. Thus, assuming that adsorption/release reactions are governed by a single reversible reaction, a coefficient k_1 governs the transfer from the liquid to the solid phase and a coefficient k_2 governs the inverse process. Also, the migration of metals to the deep sediment is included. Thus, metals deposited on the sediment surface will be buried by particle deposition and will migrate below the mixed sediment layer which directly interacts with the dissolved phase. This effect may be easily treated as a decay process with constant λ_{burial} given by (Periáñez, 2008):

$$\lambda_{\text{burial}} = \frac{\text{SR}}{\rho_s L} \tag{1}$$

where L is the sediment mixing depth (the distance to which the dissolved phase penetrates the sediment), ρ_s is the sediment bulk density (dry mass divided by wet volume) and SR is the sedimentation rate provided by the sediment transport sub-model.

It is known that adsorption depends on the surface of particles per water volume unit at each point and time. This quantity has been denoted as the exchange surface (Periáñez, 1999, 2000, 2002). Thus, the kinetic coefficient k_1 is written as:

$$k_1 = \chi(S_m + S_s\delta_b) = k_1^m + k_1^s \tag{2}$$

where S_m and S_s are the exchange surfaces for suspended matter and bottom sediments respectively (dimensions $[L]^{-1}$) and χ is a parameter with the dimensions of a velocity denoted as the exchange velocity (Periáñez, 1999, 2000, 2002). The delta function is introduced to take into account that only the deepest water layer interacts with the bed sediment. Thus $\delta_b = 1$ for the deepest layer and $\delta_b = 0$ elsewhere.

Assuming spherical particles, the exchange surfaces are written as (see references cited above):

$$S_m = \frac{3m}{\rho R} \tag{3}$$

and

$$S_s = \frac{3Lf\phi(1-p)}{R\psi} \tag{4}$$

where R and ρ are particle radius and density respectively, m is the suspended matter concentration, f is the fraction of fine particles in the sediment, p is sediment porosity and ϕ is a correction factor that takes into account that part of the sediment particle surface may be hidden by other sediment particles. Finally, ψ is the thickness of the deepest water layer. This formulation has been successfully used in all modelling works cited above. Real particles are not spheres, but with this approach it is possible to obtain an analytical expression for the exchange surface (Duursma and Carroll, 1996). The kinetic coefficient k_2 is considered to be constant.

The equation that gives the time evolution of metal concentration in the dissolved phase, C_d, is:

$$\frac{\partial C_d}{\partial t} + u\frac{\partial C_d}{\partial x} + v\frac{\partial C_d}{\partial y} + w\frac{\partial C_d}{\partial z} = A\left(\frac{\partial^2 C_d}{\partial x^2} + \frac{\partial^2 C_d}{\partial y^2}\right) + \frac{\partial}{\partial z}\left(K\frac{\partial C_d}{\partial z}\right) - k_1 C_d + k_2 m C_s + \delta_b k_2 \frac{L\rho_s \phi f A_s}{\psi} \tag{5}$$

where C_s and A_s are, respectively, the concentrations of metals in suspended matter and bottom sediments. u, v and w are water velocities along the x, y and z axis and A and K are, respectively, the horizontal and vertical diffusion coefficients.

The equation that gives the time evolution of metal concentration in suspended matter is:

$$\frac{\partial (mC_s)}{\partial t} + u\frac{\partial (mC_s)}{\partial x} + v\frac{\partial (mC_s)}{\partial y} + (w - w_s)\frac{\partial (mC_s)}{\partial z} = A\left(\frac{\partial^2 (mC_s)}{\partial x^2} + \frac{\partial^2 (mC_s)}{\partial y^2}\right) + \frac{\partial}{\partial z}\left(K\frac{\partial (mC_s)}{\partial z}\right) + k_1^m C_d - k_2 m C_s - \delta_b SED \tag{6}$$

where w_s is the particle settling velocity and SED is the deposition of metals from the deepest water layer to the sediment evaluated according to:

$$SED = SR\frac{C_s(b)}{\psi}. \tag{7}$$

Note that (b) means that the corresponding magnitude is evaluated at the deepest water layer.

The equation for the temporal evolution of metal concentration in the bottom sediment mixed layer is:

$$\frac{\partial A_s}{\partial t} = k_1^s \frac{C_d(b)\psi}{L\rho_s f} - k_2 A_s \phi - \lambda_{burial} A_s + SED \tag{8}$$

where the deposition is now calculated as:

$$SED = SR\frac{C_s(b)}{\rho_s L f}. \tag{9}$$

The total metal content, A_p, in the sediment below the mixed depth is given by the following equation:

$$\frac{\partial A_p}{\partial t} = \lambda_{burial} L\rho_s f A_s. \tag{10}$$

2.4. Numerical solution and parameters

The topography of the GoC was obtained from the NOAA (US National Ocean and Atmosphere Administration) GEODAS database, available on-line, with a resolution of 2 min in both longitude and latitude. The grid consists of 64×136 cells, extending from −8° to −5.9° in longitude and from 33° to 37.5° in latitude. Fifty vertical levels are considered, with increasing thickness from the sea surface to the bottom.

All the equations were solved using explicit finite difference schemes. In particular, the scheme described in Periáñez (2005a) is used in the 2D barotropic hydrodynamic model. In the 3D baroclinic model the scheme in Kowalick and Murty (1993) is applied. The second order accuracy MSOU (Monotonic Second Order Upstream) advection scheme (Vested et al., 1996) is applied for all advective terms and a second order scheme is used for diffusion as well (Kowalick and Murty, 1993).

Time-step in the different sub-models is selected with care to assure that stability conditions are satisfied. A time-splitting procedure was used to treat the water–sediment metal interactions. This is essentially the same as in hydrodynamic models, when time-splitting is used to solve the external and internal modes. The procedure is required because a very restrictive stability condition is introduced by such interaction terms (Periáñez, 2005a). Essentially, it consists of using a smaller time step to solve water–sediment metal interactions. Thus, for each advection/diffusion time step, a number of smaller steps are needed to solve metal partition.

Some open boundary conditions must be provided. In the barotropic model, tidal surface elevations and phases are specified along the open boundaries of the computational domain from Schwiderski (1980a,b). A radiation condition is applied to the water velocity component that is normal to the open boundary (Jensen, 1998). The equations are integrated, starting from rest, until stable oscillations are obtained. Then tidal analysis is carried out and tidal constants are stored in files. In the case of the 3D baroclinic model, water velocities are specified along the Strait of Gibraltar from the average inflow (into the Mediterranean) of Atlantic Water and deep outflow (from the Mediterranean to the Atlantic) of Mediterranean water. Water temperature and salinity along the open boundaries are specified from the NOAA WOA05 (World Ocean Atlas 2005), available on-line. Summer values are used since sampling campaigns were carried out in this season. The 3D model is again started from rest and a wind stress of 0.045 N/m^2, directed to the south, is applied. It corresponds to the summer characteristic value (Machín et al., 2006). Residual currents are stored in files that will be later read by the sediment and metal transport sub-models.

A summary of parameters involved in the models is given in Table 1. Suspended particles (diameter <63 μm) are characterized by a mean size that is considered to be representative of suspended matter in this environment. The particle size controls, through Stoke's law, the settling velocity of particles and, as a consequence, affects the sedimentation rate as well. It also affects the adsorption of metals from the dissolved phase (Eqs. (3) and (4)). The value used for particle diameter was 8 μm. Freitas and Abrantes (2002) have found that particles with diameter <10 μm are dominant in all water masses in the Gulf of Cadiz. Moreover, this is the same value selected for a model of the Alborán Sea (Periáñez, 2008) after a sensitivity analysis (the GoC reflects the Alborán Sea since surface waters in the first flow into the second and Mediterranean waters flow, in the deep layer, from the Alborán Sea into the GoC). Finally, the selected value is also consistent with Liu et al. (2002b), who used a radius of 2.5 μm to describe fine silts in their model. Of course, it would be convenient to have a detailed particle size spectra and then using several particle classes (Periáñez, 2005b), but it is not available in current literature.

The critical deposition stress typically ranges between 0.04 and 0.1 N/m^2 (Tattersall et al., 2003), while the critical erosion stress

Table 1
Summary of model parameters.

Parameter description	Value	Source
Water kinematic viscosity	$\nu = 1.064\times10^{-6}$ m^2/s	Standard value
Vertical diffusion coefficient	K = variable	Turbulence equation
Horizontal diffusion	$A = 2.0$ m^2/s	Dick and Schonfeld (1996)
Sediment mixing depth	$L = 0.1$ m	Periáñez (2000, 2003)
Particle density	$\rho = 2600$ kg/m^3	Standard value
Particle radius	$R = 4.0$ μm	Freitas and Abrantes (2002)
Fraction of small particles in sediment	f = variable	Gonzalez et al. (2007)
Correction factor	$\phi = 0.1$	Periáñez (2000, 2003); Periáñez et al. (2005)
Sediment porosity	$p = 0.5$	Periáñez (2008) (similar value)
Erodability	$E = 1.6\times10^{-3}$ kg/m^{2}s	Tattersall et al. (2003)
Critical erosion stress	$\tau_{ce} = 1.0$ N/m^2	Tattersall et al. (2003)
Critical deposition stress	$\tau_{cd} = 0.06$ N/m^2	Tattersall et al. (2003)
Desorption kinetic coefficient	$k_2 = 1.16\times10^{-5}$ s^{-1}	Nyffeler et al. (1984)
Zn distribution coefficient	$k_d = 7.0\times10^4$	IAEA (2004)
Ni distribution coefficient	$k_d = 2.0\times10^4$	IAEA (2004)
Cu distribution coefficient	$k_d = 2.6\times10^4$	Calibration

In the cases of E and the critical stresses for erosion and deposition, the selected values correspond to intermediate values within their range of variation commonly found in literature. A reference (Tattersall et al., 2003) is given as an example.

ranges 0.1–1.5 N/m^2 (Tattersall et al., 2003). In the present application intermediate values of 0.06 and 1.0 N/m^2 have been taken for the critical deposition and erosion stresses respectively, as in the Alborán Sea model described in Periáñez (2008). The erodability constant is fixed as $E = 1.6\times10^{-3}$ kg/m^{2}s. This parameter typically varies between 2×10^{-4} and 3×10^{-3} kg/m^{2}s (Tattersall et al., 2003). The fraction f of fine particles in bed sediments must be defined over the model domain. This information has been compiled from Hernández-Molina et al. (2006) and Gonzalez et al. (2007). Schematically, sand and sandy mud dominate to a depth of 30 m. The middle shelf, to a depth of 100 m, is characterized by an extensive mud belt. Finally, outer sediments below 100 m are dominated by mixtures of sand and clay.

Suspended matter concentrations in the three main rivers (Fig. 1) have been defined. Of course, these magnitudes present seasonal (and at a shorter scale as well) variations. However, representative mean values have been used for the present application. In the Odiel–Tinto estuary, the mean value measured in Periáñez et al. (1996) has been used: 30 g/m^3. The mean value measured by Gómez-Parra et al. (2000), 120 g/m^3, was selected for the Gualdalquivir estuary. Finally, in the Guadiana estuary, a mean value of 30 g/m^3 is in agreement with Machado et al. (2007) and with the empirical relation given for this estuary by Wolanski et al. (2006).

The sediment transport sub-model is run until steady particle distribution and SR are obtained. The model is forced by residual currents provided by the 3D baroclinic model. Instantaneous tidal currents are used only to calculate the bed stress. This approach has been made since the model has been run to simulate the dispersion of a passive tracer with and without tides (of course residual circulation is considered in both cases), and differences in the tracer concentration fields between both simulations could not be appreciated (the simulated time was just a few months). Suspended particle concentrations and sedimentation rates are stored in files that are read by the metal transport model.

Table 2
Values of river discharge metal concentrations (nM).

Metal	Guadiana	Guadalquivir	Odiel–Tinto
Cu	42	58	214
Ni	20	43	67
Zn	49	33	129

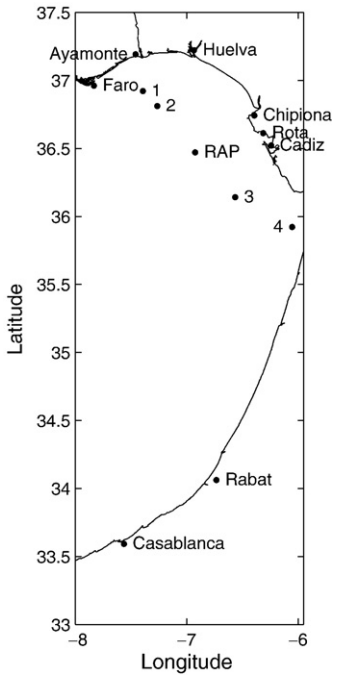

Fig. 2. Map of the GoC showing all locations mentioned in the text.

The vertical diffusion coefficient is taken equal to the vertical eddy viscosity, which is provided by the turbulence equation included in the 3D baroclinic model. The horizontal diffusion coefficient depends on the horizontal grid spacing. Following Dick and Schonfeld (1996):

$$A = 0.2055 \times 10^{-3} \Delta x^{1.15}. \quad (11)$$

The present grid resolution (2 min) gives $A = 2.0$ m^2/s.

The model has been applied to simulate the dispersion of three metals: Zn, Cu and Ni. Values for parameters describing metal transport are summarized in Table 1 too.

The correction factor ϕ has been fixed as 0.1 according to previous modelling works (Periáñez, 2000, 2003; Periáñez et al., 2005). An intermediate value of 0.5 was used for the sediment porosity. Indeed, it is 0.6 in the Alborán Sea model according to measurements (Periáñez, 2008). The sediment mixed depth is $L = 0.1$ m (Periáñez, 2000, 2003).

The so-called equilibrium distribution coefficient, k_d, describes the partition of a tracer between the dissolved and solid phases at equilibrium (Duursma and Carroll, 1996):

$$k_d = \frac{C_s}{C_d} \quad (12)$$

where C_s and C_d are tracer concentrations in the solid and dissolved phases respectively. This parameter is of course depending on the

Table 3
Established, index *obs*, (NOAA, 1982) and computed, index *comp*, amplitudes (A, cm) and phases (g, deg) of tidal elevations at several locations indicated in Fig. 2.

Station	M_2				S_2			
	A_{obs}	g_{obs}	A_{comp}	g_{comp}	A_{obs}	g_{obs}	A_{comp}	g_{comp}
Faro	92	94	99	68	32	125	36	91
Chipiona	102	54	104	62	41	82	38	85
Rota	105	52	103	62	37	78	38	85
Cadiz	100	87	99	61	37	110	36	83
Ayamonte	100	59	101	65	32	88	36	89
Huelva	102	56	105	65	38	82	38	88
Casablanca	99	56	92	53	35	81	36	77
Rabat	88	59	98	57	35	83	36	78

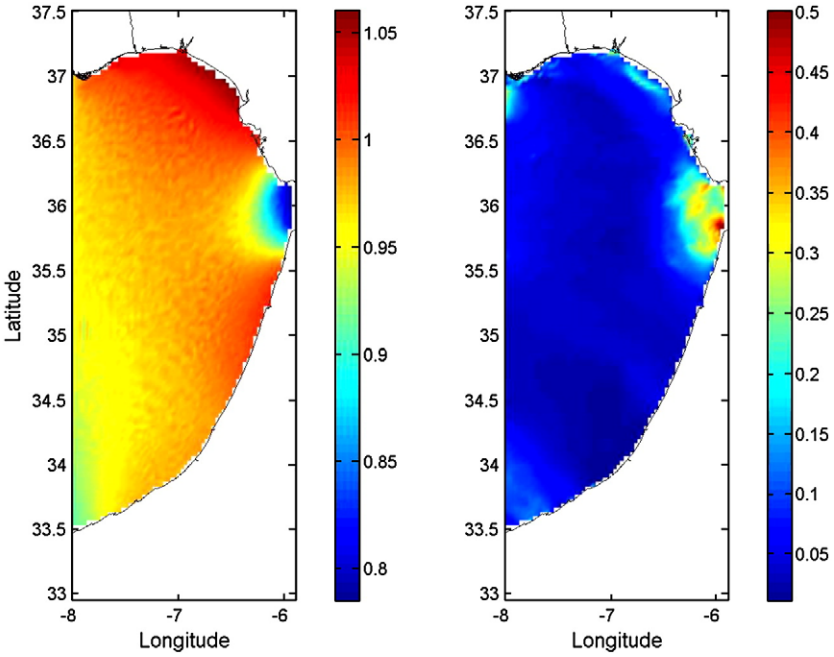

Fig. 3. Amplitude of the M_2 tide in m (left) and current amplitude in m/s (right).

tracer geochemical behaviour and on environmental conditions, thus it is a site-specific parameter.

As described before (Nyffeler et al., 1984), k_2 is very similar even for elements with a rather different geochemical behaviour, being χ (see Eq. (2)) the essential parameter describing the tracer geochemical behaviour. Thus, the same value is given to k_2 for Ni, Zn and Cu, which is $k_2 = 1.16 \times 10^{-5}\ s^{-1}$. This value has been successfully used in earlier simulations in the Odiel–Tinto estuary (Periáñez et al., 2005) and in the Strait of Gibraltar–Alborán Sea (Periáñez, 2008) for several elements (Ra, Cs, Pu). It was measured for Cs by Nyffeler et al. (1984).

The exchange velocity for each metal is obtained from the equation relating this parameter with k_2 and its corresponding equilibrium distribution coefficient, k_d (Periáñez, 2005a):

$$k_d = \frac{\chi}{k_2}\frac{3}{\rho R}. \tag{13}$$

The k_d mean values recommended by the International Atomic Energy Agency (IAEA, 2004) for coastal waters have been used. This procedure has been widely used before (Periáñez 1999, 2000, 2003, 2008).

Distribution coefficients are given in Table 1. Nevertheless, they may vary in more than one order of magnitude depending on environmental conditions. Consequently, the model sensitivity to this parameter has been studied and results are presented below (Section 3.3.2). The IAEA does not provide k_d values for Cu, thus in the case of this metal it had to be obtained from a calibration procedure. The selected value, 2.6×10^4 is, however, of the same order of magnitude of the measured Cu k_d (Wen et al., 1999) in USA coastal waters (1.3×10^4).

Metal concentrations in the dissolved phase have been defined at the three main sources, Guadalquivir, Guadiana and Odiel–Tinto estuaries. Values, which are the same used by Beckers et al. (2007), are given in Table 2.

The metal transport sub-model is started from background dissolved concentrations, which correspond to the open Atlantic Ocean metal concentrations reported in Elbaz-Poulichet et al. (2001). The corresponding background in the solid phase is obtained from the metal k_d through Eq. (12). Equations are integrated until steady metal distributions are obtained in all phases.

All the modelling work has been carried out in a sequential way. Thus, the hydrodynamic sub-model is developed first. Once that acceptable tides and residual currents are obtained, these are used to simulate sediment dynamics. Finally, metal transport is included when the sediment sub-model model has been validated.

3. Results and discussion

A brief description of the hydrodynamic and sediment transport results is given. Next, model results for metal distributions are discussed.

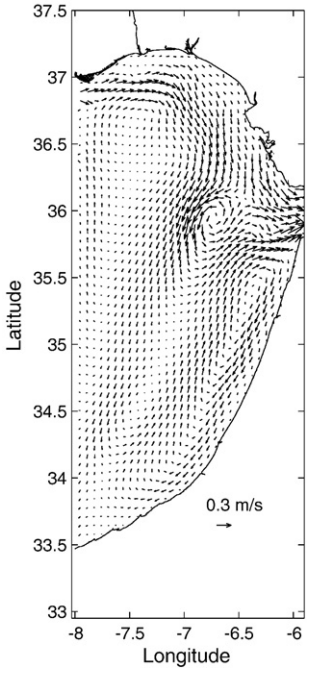

Fig. 4. Computed surface residual currents. Only one of each 4 vectors is drawn.

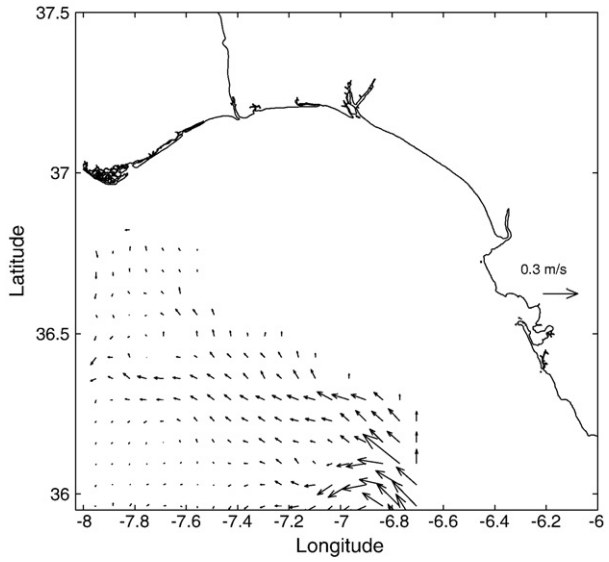

Fig. 5. Computed residual currents 590 m below the surface in the northern GoC. Only one of each 4 vectors is drawn.

3.1. Hydrodynamics

A map showing the different locations and sampling points mentioned in the paper is presented in Fig. 2. Computed tidal constants have been compared with established values for both M_2 and S_2 tides. Results are shown in Table 3, and it may be seen that, generally, there is a good agreement between both set of data. As an example, maps showing the M_2 tide amplitude and the amplitude of the tidal current are presented in Fig. 3. The amplitude of the tide is about 1 m over all the GoC, decreasing near the Strait of Gibraltar. Associated currents are weak, with amplitudes below 0.10 m/s over most of the GoC. Indeed at the RAP (Red de Aguas Profundas, Spanish Institute of Oceanography) buoy position (see Fig. 2), the M_2 barotropic tidal current is less than 0.03 m/s (García-Lafuente et al., 2006). The computed current at this position is 0.034 m/s. The current amplitude increases as approaching the Strait entrance, where currents about 0.8 m/s are produced (the color scale in Fig. 3 is limited to 0.5 m/s for more clarity). A similar behaviour is observed for the S_2 tide.

The residual surface circulation in the northern GoC is characterized by a current directed to the SE (Criado-Aldeanueva et al., 2006; García-Lafuente and Ruiz, 2007) along the Spanish coast. This circulation is a rather constant pattern during most of the year. Part of the flow enters the Strait of Gibraltar and part is deflected to the south. The residual circulation computed with the baroclinic model at the sea surface is presented in Fig. 4. The current is effectively directed to the SE over the continental shelf and part of this flow enters the Strait of Gibraltar. Maximum currents are of the order of 0.3 m/s, in agreement with García-Lafuente et al. (2006). The anticyclonic eddy at the east of Faro (see Fig. 2) has been described by Machín et al. (2006). Also, the cyclonic eddy in front of the Strait of Gibraltar appears clearly in the models of Beckers et al. (2007) and Peliz et al. (2007). These last authors have attributed it to the strong convergence occurring in this area.

Below the surface, the Mediterranean waters flow into the Atlantic and mainly direct to the NW (Serra et al., 2005; Ambar and Howe, 1979; Johnson et al., 2002). As an example, the computed circulation 590 m below the surface is presented in Fig. 5. Only the northern part of the GoC is shown to appreciate details more clearly. These currents are in agreement with the geostrophic velocities below 400 m, referenced to 300 m, provided by Criado-Aldeanueva et al. (2006) and with the calculations by Peliz et al. (2007) for summer. Water velocity is higher close to the Strait and then slows to about 0.1 m/s, in agreement with Ambar and Howe (1979).

Temperature and salinity profiles in the water column calculated by the model have been compared with those obtained from observations carried out under the TOROS project (Elbaz-Poulichet et al., 2001) in summer 1997. Examples for 4 points shown in Fig. 2 may be seen in Fig. 6. There is an acceptable agreement between model results and experimentally obtained vertical profiles of T and S.

Finally, two vertical south–north sections of water salinity are presented in Fig. 7, at longitudes of −6.87° and −6.05°. In the first

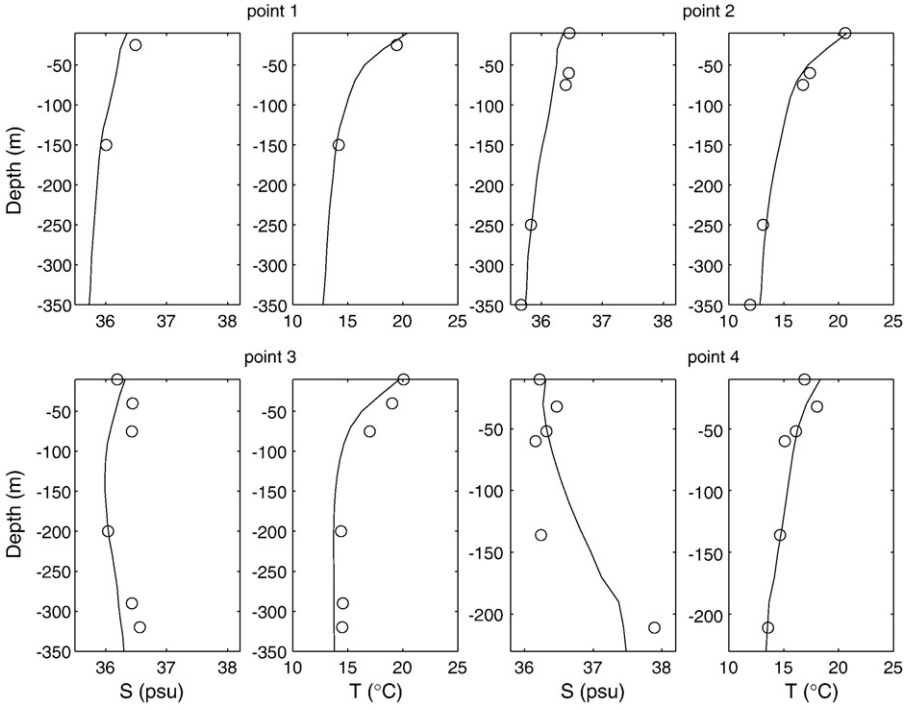

Fig. 6. Computed (lines) and measured (points) salinity and temperature profiles in points indicated in Fig. 2.

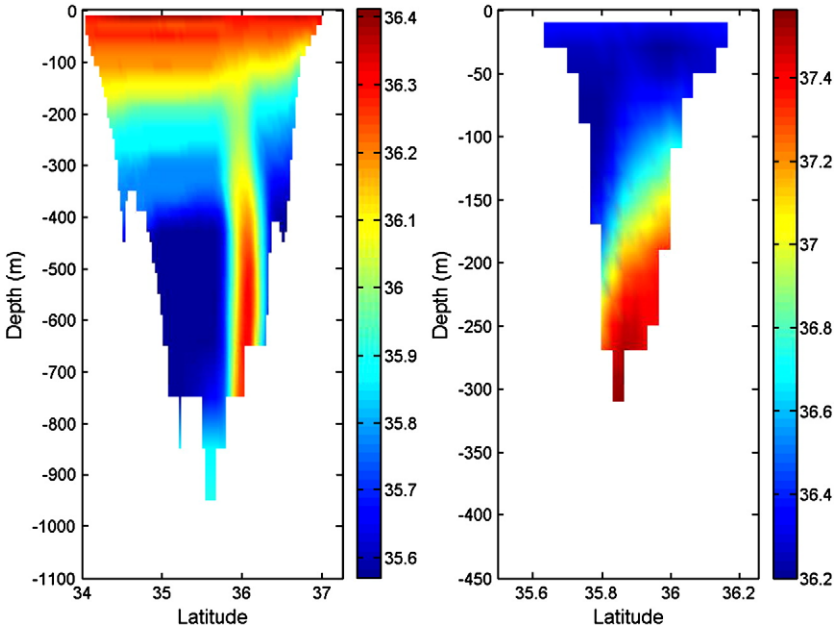

Fig. 7. Vertical south–north salinity sections at longitudes −6.87° and −6.05° (left and right respectively).

case, the core of more dense Mediterranean water is clearly seen, with the salinity maximum below 600 m. This flow is aligned with the Spanish continental slope, in agreement with Jungclaus and Mellor (2000) and Peliz et al. (2007). Close to the Strait, the situation may be characterized as a two-layer exchange flow, with the interface tilted down southward (Jungclaus and Mellor, 2000).

Although seasonally averaged values have been used for open boundary conditions and wind stress, the main features of water circulation in the GoC are, generally speaking, reproduced by the model for the considered season.

3.2. Suspended matter

As expected, the river-discharged suspended matter is transported to the southeast along the Spanish coast, which is the residual current direction in this area of the GoC. As widely discussed (Gonzalez et al., 2007), there is a dominant eastward transport throughout the entire northern GoC. Some authors (Lobo et al., 2004) have postulated the existence of some westward transport of sediments released by the Guadalquivir River in the inner shelf, although little indication of it has been found in other works (Gonzalez et al., 2007).

Maps of suspended matter concentrations at the surface and in the deepest water layer are presented in Fig. 8. Logarithmic scale is used to appreciate differences. The suspended particle plumes produced by the three rivers can be clearly seen in the maps. Indeed, concentrations of the order of 10 g/m^3 are obtained near the river mouths. Concentrations of the order of 10^{-1} g/m^3 are obtained in part of the northern GoC and much smaller values are apparent to the south. Computed surface particle concentrations are in agreement, by order of magnitude, with measured surface concentrations. Indeed, concentrations of the order of 10^{-1} g/m^3 have been measured at the surface in the northern GoC (Palanques et al., 1986–1987). Also, concentrations in the range 20–45 g/m^3 have been detected in the Guadiana River plume (Cravo et al., 2006) over a narrow area (<10 km from the coast). In the deepest water layer concentrations are slightly higher than at the surface over most of the northern GoC, in agreement with Palanques et al. (1986–1987). In some areas as the Strait of Gibraltar and the Spanish continental slope, concentrations are more significantly enhanced in the deep water. This is probably due to erosion produced by stronger tidal currents (in the area of the Strait) and also produced by the Mediterranean water current.

A south–north section of suspended matter concentrations at the Atlantic entrance of the Strait of Gibraltar (longitude −6.10°) is shown in Fig. 9. The plume of particles released by the rivers may be seen in surface waters at the northern area of the section. Maximum concentrations, however, are obtained in Mediterranean waters, at depth about 200 m and along the Spanish continental slope. This indicates that erosion is occurring in this area, as commented above.

Computed net sedimentation rates (not shown) are larger, as expected, in the vicinity of the river mouths, where they are of the order of 10^{-3} g/cm^2year. Much smaller values are obtained far from the river discharge influence. In particular, there is a region where no sedimentation occurs at the west of the Strait of Gibraltar. This is due to the strong currents in the Mediterranean outflow water (Fig. 5), which keep particles in suspension. Nevertheless, all these results have to be interpreted with care since several approximations have implicitly been made in the model: there are variations in water exchanges through the Strait of Gibraltar, as already discussed in previous modelling works (Periáñez, 2008). Of course, these variations will affect the SR. Although constant suspended matter concentrations have been defined in the three estuaries, there will also be seasonal variations depending on pluviometry, for instance. Only fine particles are considered in the model, and bed load transport is neglected. This approximation will lead to lower sedimentation rates. The same occurs due to the fact that organic particles are not included. Finally, atmospheric deposition events of particles coming from the Sahara Desert (Fabres et al., 2002) have not been considered in the model since they cannot be easily quantified (Periáñez, 2008). It must be taken into account that suspended particles will affect metal transport only close to the coast, given the extremely low suspended matter concentrations which are measured offshore (Palanques et al., 1986–1987), and river supply is the main sediment source in this coastal area.

3.3. Heavy metal transport

3.3.1. Metal distributions

As commented before, the model has been applied to simulate the transport of three metals in the GoC: Zn, Cu and Ni. Pathways of metals are essentially the same as for suspended particles. Thus, they are transported to the east, along the Spanish coast, until the Strait of Gibraltar.

The concentrations of several metals have been measured in the fine sediment fraction (<63 μm) along the Spanish coast from the

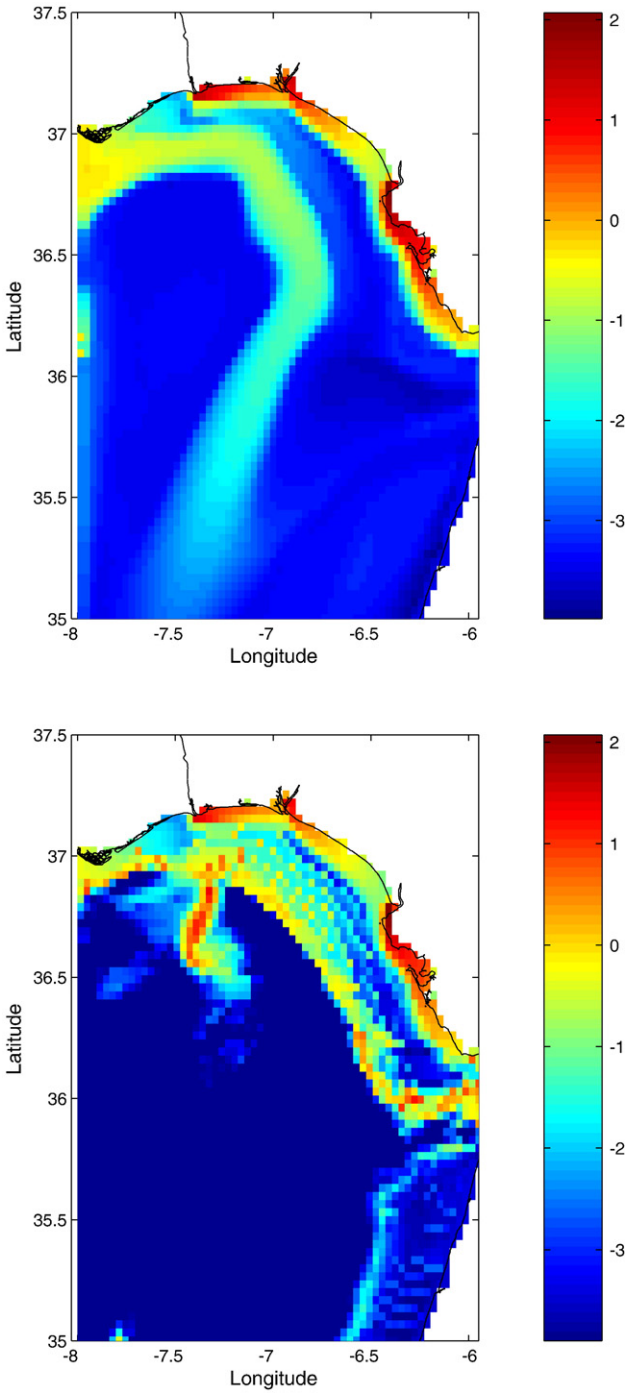

Fig. 8. Computed surface suspended matter concentrations (g/m^3) in logarithmic scale at the surface (top) and bottom (down) of the water column.

Guadiana to the Guadalquivir mouths (Sainz and Ruiz, 2006; Morillo et al., 2004) and also at some points closer to the Strait of Gibraltar (Riba et al., 2002). Samples were collected at an approximate distance of 500 m from the shoreline. A comparison of measured (points) and computed (lines) metal concentrations along the northern coast of the model domain can be seen in Fig. 10. In general, there is a good agreement between the measured and calculated concentrations, although in the case of Ni the model produces a concentration peak in the area of the Odiel–Tinto mouth that is not apparent in measurements. This discrepancy could be caused, at least partially, by a different nature of particles released from this river, which affects the partition on Ni (although does not in the cases of Zn and Cu). Also, it is

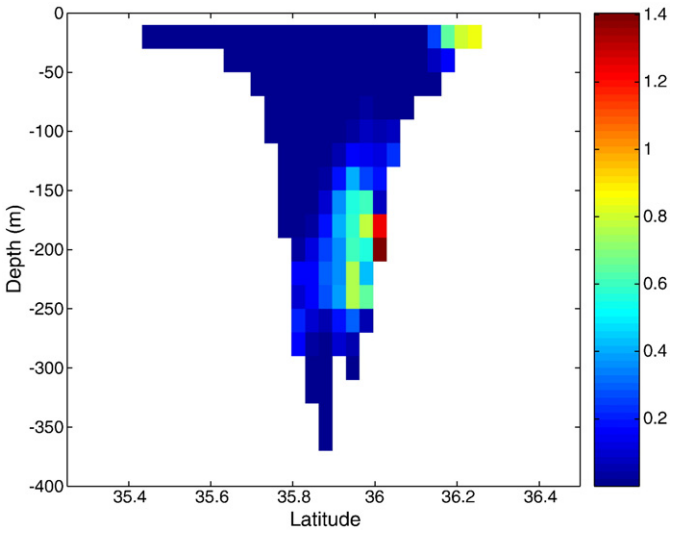

Fig. 9. Vertical south–north section of suspended matter concentrations (g/m^3) at the Atlantic entrance of the Strait (longitude −6.10°).

possible that the source term is overestimated in the case of Ni for the Odiel–Tinto River. A clear conclusion cannot be obtained.

Metal concentrations are very low westward from the Guadiana River. There is an increase in concentrations here since, as has already been mentioned, the three rivers drain the Iberian Pyrite Belt. Maximum concentrations exist in the mouth of the Odiel–Tinto rivers. Although river flows are much smaller than those of the Guadiana and Guadalquivir, Odiel–Tinto rivers are considerably more contaminated (Gonzalez et al., 2007) and, indeed, they have been recognized as the main source of metals along the coast (Morillo et al., 2004).

There is not an appreciable metal enhancement in the area of the Guadalquivir mouth (except in the case of Ni where both measurements and calculations show such an enhancement). Metal concentrations at the east of the Odiel–Tinto rivers decrease much slower than at the west of the Guadiana River, which is due to the residual currents in the shelf, which flow towards the Strait of Gibraltar. Indeed, it has already been found (Elbaz-Poulichet et al., 2001) that coastal waters transport dissolved metals (which contaminate bed sediments as metals travel over them) from the Odiel–Tinto rivers to a

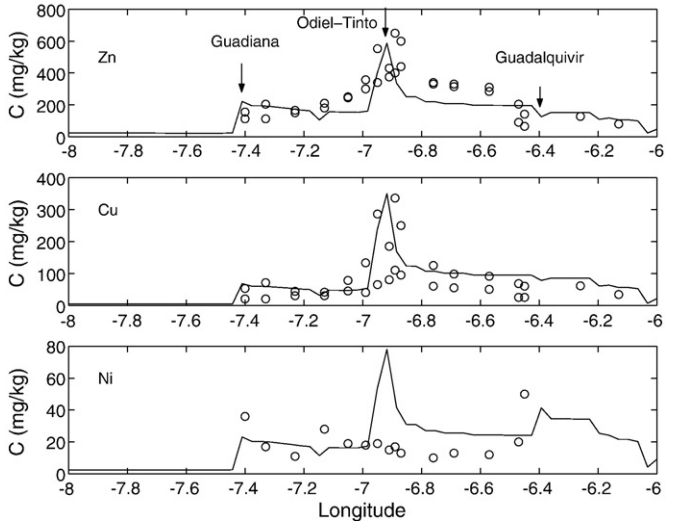

Fig. 10. Measured (circles) and computed (lines) metal concentrations in sediments along the northern coast of the model domain. The three arrows indicate the location of the Guadiana, Odiel–Tinto and Guadalquivir mouths (from left to right).

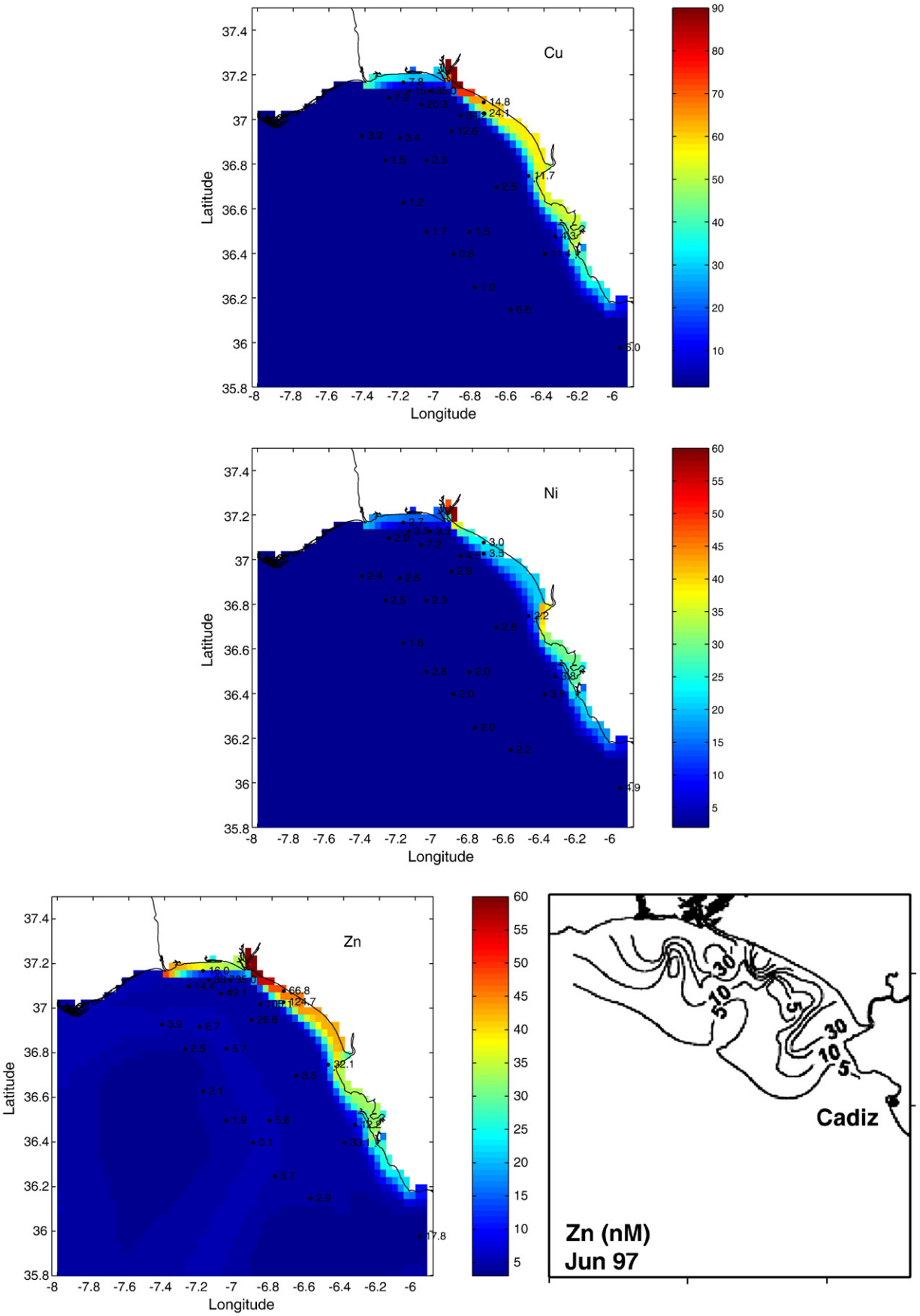

Fig. 11. Measured and computed (color scale) metal concentrations (nM) in surface waters of the northern GoC. A contour plot showing surface dissolved Zn concentrations (nM) in June 1997 from experimental data (from Achterberg et al., 1999) is also shown (right of the bottom row).

distance of more than 200 km. Moreover, it has been found that these rivers constitute a source of natural radionuclides into the Mediterranean through the Strait of Gibraltar (Gascó et al., 2002).

Concentrations of dissolved metals have been measured in the northern GoC in the frame of the TOROS project (Elbaz-Poulichet et al., 2001) in summer 1997. A comparison between measured and computed surface concentrations may be seen in Fig. 11. In all cases, dissolved metal concentrations decrease quickly with distance from the coast. The highest concentrations are obtained in the mouth of the Odiel–Tinto rivers, obviously as in the case of bed sediments. The plume of dissolved metals reaches the Strait of Gibraltar, as has been obtained from measurements and has been commented above (Elbaz-Poulichet et al., 2001; Gascó et al., 2002). The maps presented in Fig. 11 are in good agreement with contour plots obtained from empirical data (Achterberg et al., 1999), which show essentially the same banded structure. As an example, such contour plot is presented as well in Fig. 11 for the case of Zn. It may be clearly seen that, effectively, the impacts from river outflow are restricted to a narrow band along the shore. Samples were not collected in the coastal area from Cadiz to the Strait, thus the impact is apparently restricted in the experimental contours of Fig. 11 to the zone located to the north of Cadiz.

Dissolved metal concentrations deeper in the water column (not shown) are rather uniform (for instance in the range 3–5 nM for the case of Zn) since deeper waters (depth > 50 m) are not affected by river discharges. Indeed, it has been found that the main core of metal enriched water extends to about the 50 m isobath (Achterberg et al., 1999). Along Spain, this isobath is typically some 20 km from the shore.

Vertical south–north sections of dissolved metal concentrations (Cu and Ni) at the Atlantic entrance of the Strait (longitude −6.10°) are shown in Fig. 12. In both cases, the metal plumes coming from the rivers are clearly visible above some 50 m depth in the northern part of the section. Ni concentration in the Mediterranean water is higher than in water above it. The inverse situation is observed for Cu. These results are in agreement with data presented in Gómez (2003), which show this effect.

Computed background metal concentrations in suspended matter are of the order of 10^2 nmol/g, 10^3 nmol/g and 10^2 nmol/g for Cu, Zn and Ni respectively. In Atlantic Shelf waters (English Channel) particulate Zn concentrations range 1160–4900 nmol/kg (Cobelo-García et al., 2005). In the case of Cu this range is 60–380 nmol/kg. Information was not found for Ni. Computed particulate backgrounds seem to be in reasonable agreement with measurements in the Atlantic Ocean.

Model results, however, have to be interpreted with care (as commented before for suspended matter transport) since river plumes of suspended particles and hence contaminants are sensitive to changes in wind speed and direction as well as they depend on pluviometry. Moreover, other meteorological conditions, such as atmospheric pressure differences between the Atlantic and Mediterranean, can induce flow variations through the Strait of Gibraltar. East winds, which may be particularly strong in the Strait during spring and summer, can inhibit the water input from the GoC into the Mediterranean and consequently retain pollutants in the GoC. On the other hand, organic particles are not included and they are thought to play a specific role on sorption reactions on suspended matter since it might provide sorption sites due either to their chemical structure or because of their polar (or non-polar) character (Duursma and Carroll, 1996). Finally, other sources of metals in the GoC have not been included in this study, as such related to the intensive industrial activity in Cadiz Bay. These effects make the comparison of computed metal concentrations in the water column with the corresponding measurements specially difficult (as already discussed by Dyke, 2001). However, bed sediments integrate all this variability and the generally good behaviour of the model in reproducing sediment contamination gives some confidence on the model.

3.3.2. Sensitivity analysis

The main parameter which describes the geochemical behaviour of metals is the exchange velocity χ, obtained from the equilibrium

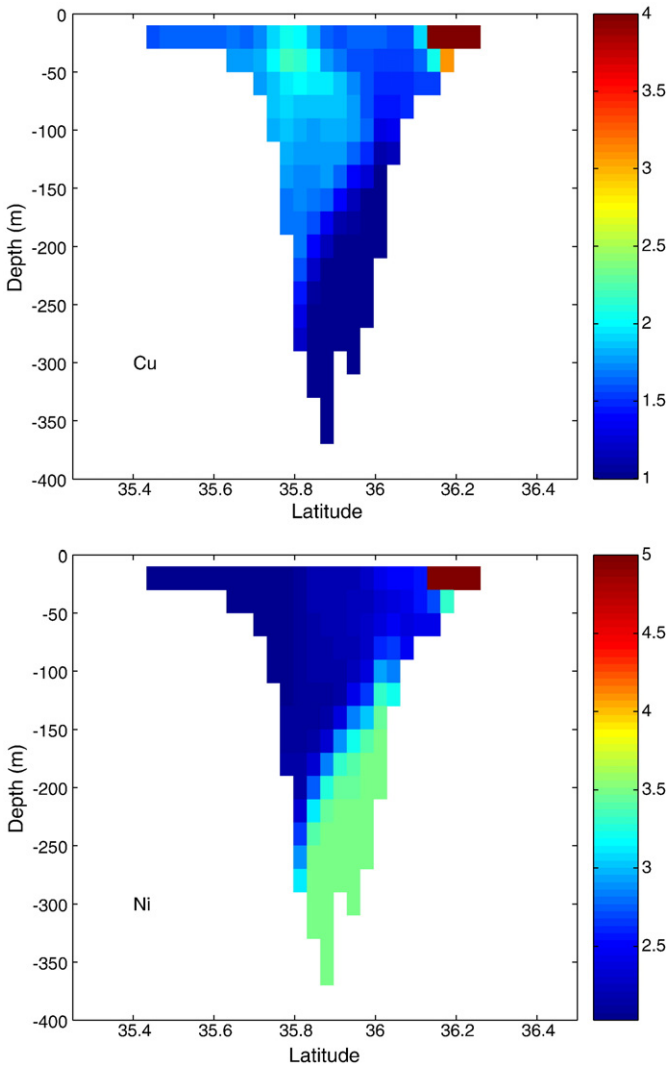

Fig. 12. Vertical south–north sections of dissolved metal concentrations (nM) for Cu and Ni at the Atlantic entrance of the Strait (longitude −6.10°).

distribution coefficient k_d through Eq. (13), as already described. The model sensitivity to changes in this last parameter has been investigated since the k_d is poorly defined and presents a high natural variability depending on environmental conditions (mainly pH, temperature and salinity, although other parameters as light intensity may be relevant as well).

Obviously, a higher k_d means that the substance has a higher affinity to be fixed to the solid phase and vice versa. Thus, surface sediment metal concentrations are linearly correlated with the k_d, as should be expected from the model formulation.

The distribution of metals in coastal sediments obtained with several k_d values have been computed and are presented in Fig. 13a in the case of Zn. The value 2.0×10^5 has been measured in coastal waters of the USA (Wen et al., 1999). A smaller value, by one order of magnitude, has also been tested (2.0×10^4). Effectively, too high metal concentrations, when compared with empirical data, are obtained with 2.0×10^5. On the other hand, concentrations are too low if a k_d of 2.0×10^4 is used. The best agreement between measured and computed metal concentrations is obtained with the k_d recommended by the IAEA (2004), which is indicated in Fig. 13a as the nominal simulation.

The k_d value in the case of Cu was obtained from a calibration exercise. Thus, the k_d value was changed, by trial and error, until a

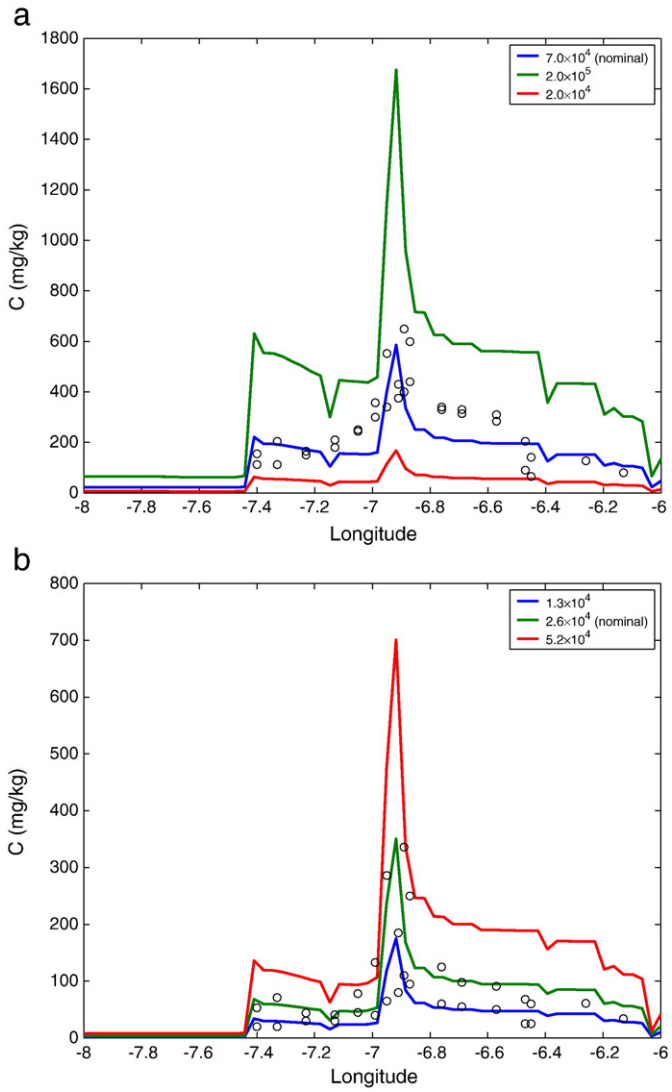

Fig. 13. Model sensitivity to the distribution coefficient. (a): Zn. Results in Fig. 10 are presented for three k_d values. The nominal simulation corresponds to $k_d = 7 \times 10^4$. (b): Cu. In this case the nominal simulation corresponds to $k_d = 2.6 \times 10^4$.

good agreement between model results and observation was obtained. A summary of this exercise may be seen in Fig. 13b. In general, the best agreement was obtained with $k_d = 2.6 \times 10^4$. The value measured by Wen et al. (1999), 1.3×10^4, produces sediment Cu concentrations lower than measured values, and, on the other hand, too high Cu concentrations are computed if 5.2×10^4 is used. The sensitivity analysis is not shown in the case of Ni, but similar results are obtained. The IAEA (2004) k_d value, which is also similar to the value measured by Wen et al. (1999), produces better results than if it is reduced or increased by a factor two.

The sensitivity of the formulation of the water–sediment metal interaction processes to other parameters as particle size and density, sediment mixing depth, fraction of small particles and the correction factor ϕ has already been studied in detail (Periáñez, 2002, 2004) and will not be repeated here.

4. Conclusions

The transport of heavy metals in the GoC has been studied by means of numerical modelling. Water circulation has been obtained from two models working on the same domain. A 2D depth-averaged barotropic model provides tides. The residual circulation is obtained from a full 3D baroclinic model. This model is forced, at its open boundaries, by climatological data.

Computed tides have been compared with observations, being in good agreement with these. The residual circulation shows the well-known southeast circulation along the Spanish coast and the deeper Mediterranean water flow directed from the Strait of Gibraltar to the northwest. Computed vertical profiles of temperature and salinity have been compared with observed profiles at some points in the GoC. Both set of data are, in general, in good agreement.

Results of the hydrodynamic models are used by a 3D sediment transport model which includes advection/diffusion of particles, settling, deposition and erosion of the sediment. The settling velocity is obtained from Stoke's law, and deposition and erosion are described using standard equations which include the erodability constant concept as well as erosion and deposition critical stresses. The total bed stress is obtained from the tidal and residual currents at the bottom. Sources of particles are the three main rivers discharging in the GoC: Guadiana, Odiel–Tinto and Guadalquivir. Only the lithogenic particle fraction is considered and bed-load transport is not included in the model. The model shows that the river plumes are directed to the east, transported by the residual currents as should be expected. Suspended particle concentrations provided by the model are, generally speaking, in agreement with observations.

The three rivers mentioned above constitute a source of heavy metals to the GoC since they drain the Iberian Pyrite Belt. A model which simulates metal transport has been developed. It uses computed currents and suspended particle concentrations and sedimentation rates. Metal exchanges between the dissolved phase, suspended matter and bed sediments are included. These processes are formulated using kinetic transfer coefficients. The model has been applied to three metals: Zn, Cu and Ni. Measured metal concentrations in bed sediments collected along the Spanish coast are in agreement with calculations. Levels of computed dissolved metal concentrations in surface water are also in agreement with measurements. The path followed by metals is the same as suspended particles, thus a dominant southeast transport is observed. Indeed, metal plumes reach the Strait of Gibraltar and these rivers constitute a source of heavy metals into the Mediterranean Sea. The behaviour of the three studied metals is similar since so they are their corresponding distribution coefficients, which vary within one order of magnitude. The described model, once it has been checked that provides realistic results, may be used as a predictive tool to assess the effects of accidental or deliberate metal discharges into the GoC from rivers or other sources.

With respect to future improvements in the model, it does not seem realistic, at this moment, to go deeper into biogeochemical processes (effects of pH, redox conditions, bioturbation, organic particles and biota etc) due to the lack of field data which could be used to parameterize such processes and also to test model results. Nevertheless, it would of course be desirable to improve the model in such directions, specially with respect to the inclusion of organic particles. On the other hand, it would be interesting to modify the model in such a way that could be run under non-steady conditions. The objective would be to study the effects in metal distributions of seasonally changing water current fields and of changes in particle and heavy metal discharges from rivers originating, for instance, from heavy rain episodes.

Acknowledgements

Work supported by the Research Project of Excellence RNM-419 *Técnicas Ultrasensibles para la Determinación de Radionucleidos en Muestras Ambientales*, Junta de Andalucía, Spain. The author is indebted to the Spanish Ministerio de Educación y Ciencia for a

fellowship to stay during three months at the University of Wales, Bangor, where part of this work was carried out.

Appendix A. Hydrodynamics

The depth-averaged hydrodynamic equations, used for tidal calculations, are:

$$\frac{\partial \zeta}{\partial t} + \frac{\partial}{\partial x}(Hu) + \frac{\partial}{\partial y}(Hv) = 0 \tag{14}$$

$$\frac{\partial u}{\partial t} + u\frac{\partial u}{\partial x} + v\frac{\partial u}{\partial y} + g\frac{\partial \zeta}{\partial x} - \Omega v + \frac{\tau_u}{\rho H} = A\left(\frac{\partial^2 u}{\partial x^2} + \frac{\partial^2 u}{\partial y^2}\right) \tag{15}$$

$$\frac{\partial v}{\partial t} + u\frac{\partial v}{\partial x} + v\frac{\partial v}{\partial y} + g\frac{\partial \zeta}{\partial y} + \Omega u + \frac{\tau_v}{\rho H} = A\left(\frac{\partial^2 v}{\partial x^2} + \frac{\partial^2 v}{\partial y^2}\right) \tag{16}$$

where u and v are the depth averaged water velocities along the x and y axis, h is the depth of water below the mean sea level, ζ is the displacement of the water surface above the mean sea level measured upwards, $H = h + \zeta$ is the total water depth, Ω is the Coriolis parameter ($\Omega = 2w\sin\beta$, where w is the Earth rotational angular velocity and β is latitude), g is acceleration due to gravity, ρ is a mean value of water density and A is the horizontal eddy viscosity. τ_u and τ_v are friction stresses that have been written in terms of a quadratic law:

$$\begin{aligned} \tau_u &= k\rho u\sqrt{u^2 + v^2} \\ \tau_v &= k\rho v\sqrt{u^2 + v^2} \end{aligned} \tag{17}$$

where k is the bed friction coefficient.

The full 3D hydrodynamic equations including the terms corresponding to density gradients are written in the hydrostatic and Boussinesq approximations as:

$$\frac{\partial \zeta}{\partial t} + \frac{\partial}{\partial x}\left[(h+\zeta)\int_{-h}^{\zeta} u\,dz\right] + \frac{\partial}{\partial y}\left[(h+\zeta)\int_{-h}^{\zeta} v\,dz\right] = 0 \tag{18}$$

$$\frac{\partial u}{\partial t} + u\frac{\partial u}{\partial x} + v\frac{\partial u}{\partial y} - \Omega v + g\frac{\partial \zeta}{\partial x} + \frac{g}{\rho_0}\int_z^{\zeta}\frac{\partial \rho_w}{\partial x}dz = \frac{\partial}{\partial z}\left(K\frac{\partial u}{\partial z}\right) + A\left(\frac{\partial^2 u}{\partial x^2} + \frac{\partial^2 u}{\partial y^2}\right) \tag{19}$$

$$\frac{\partial v}{\partial t} + u\frac{\partial v}{\partial x} + v\frac{\partial v}{\partial y} + \Omega u + g\frac{\partial \zeta}{\partial y} + \frac{g}{\rho_0}\int_z^{\zeta}\frac{\partial \rho_w}{\partial y}dz = \frac{\partial}{\partial z}\left(K\frac{\partial v}{\partial z}\right) + A\left(\frac{\partial^2 v}{\partial x^2} + \frac{\partial^2 v}{\partial y^2}\right) \tag{20}$$

where ρ_w is water density, ρ_0 is a reference density, and K and A are the vertical and horizontal eddy viscosities respectively.

The vertical component of the water velocity, w, is obtained from the continuity equation:

$$\frac{\partial u}{\partial x} + \frac{\partial v}{\partial y} + \frac{\partial w}{\partial z} = 0. \tag{21}$$

The water density is derived from an equation of state relating density to salinity and temperature:

$$\rho_w = \rho_0[1 - \alpha(T - T_0) + \beta(S - S_0)] \tag{22}$$

where S is salinity, T is temperature, $\alpha = 2.14\times10^{-4}$ and $\beta = 7.45\times10^{-4}$. The reference salinity is taken as $\rho_0 = 999.7$ kg/m^3 at $S_0 = 0$ and $T_0 = 10$ °C.

Water salinity is determined from an advection–diffusion equation:

$$\frac{\partial S}{\partial t} + u\frac{\partial S}{\partial x} + v\frac{\partial S}{\partial y} + w\frac{\partial S}{\partial z} = A\left(\frac{\partial^2 S}{\partial x^2} + \frac{\partial^2 S}{\partial y^2}\right) + \frac{\partial}{\partial z}\left(K\frac{\partial S}{\partial z}\right) \tag{23}$$

and a similar equation is used for temperature:

$$\frac{\partial T}{\partial t} + u\frac{\partial T}{\partial x} + v\frac{\partial T}{\partial y} + w\frac{\partial T}{\partial z} = A\left(\frac{\partial^2 T}{\partial x^2} + \frac{\partial^2 T}{\partial y^2}\right) + \frac{\partial}{\partial z}\left(K\frac{\partial T}{\partial z}\right). \tag{24}$$

Vertical eddy viscosity is determined from a 1-equation turbulence model. The equation for the turbulent kinetic energy E is:

$$\frac{\partial E}{\partial t} = K\left\{\left(\frac{\partial u}{\partial z}\right)^2 + \left(\frac{\partial v}{\partial z}\right)^2\right\} + \beta_0\frac{\partial}{\partial z}\left(K\frac{\partial E}{\partial z}\right) - \varepsilon + \frac{g}{\rho_0}K\frac{\partial \rho}{\partial z}. \tag{25}$$

The first term in the right side of the equation represents generation of turbulence by the vertical shear, the second term is diffusion of turbulence and the last term is loss of turbulence by buoyancy (conversion of kinetic energy into potential energy). ε represents dissipation of turbulence, that is written as:

$$\varepsilon = C_1 E^{3/2}/\ell \tag{26}$$

where ℓ is a mixing length and C_1 a numeric coefficient. The vertical viscosity is finally written as a function of energy as:

$$K = C_0\ell E^{1/2} + \lambda_t \tag{27}$$

where C_0 is a numeric coefficient and λ_t is a background value of viscosity, that is the minimum possible value that it may have. The values of the numeric constants appearing above are: $\beta_0 = 0.73$, $C_0 = C^{1/4}$, $C_1 = C_0^3$ and $C = 0.046$. The background viscosity is fixed as $\lambda_t = 10^{-4}$ m^2/s.

The mixing length is derived from an algebraic expression:

$$\ell = \frac{1}{1/\ell_1 + 1/\ell_2} \tag{28}$$

with

$$\ell_1 = \kappa(z + z_0 + h)e^{\beta_1\frac{z+h}{h}} \tag{29}$$

$$\ell_2 = \kappa(z_s - z) \tag{30}$$

where $\kappa = 0.4$ is the von Karman's constant, $\beta_1 = -2.0$ and z_s and z_0 are the roughness lengths of the sea surface and bottom respectively.

Appendix B. Suspended matter transport

The equation which provides the suspended matter concentration, m, is:

$$\frac{\partial m}{\partial t} + u\frac{\partial m}{\partial x} + v\frac{\partial m}{\partial y} + (w - w_s)\frac{\partial m}{\partial z} = A\left(\frac{\partial^2 m}{\partial x^2} + \frac{\partial^2 m}{\partial y^2}\right) + \frac{\partial}{\partial z}\left(K\frac{\partial m}{\partial z}\right) \tag{31}$$

where w_s is the settling velocity of suspended particles. The deposition and erosion terms are incorporated into the sea bed boundary condition of the equation. The deposition rate is written as:

$$DP = w_s m(b)\left(1 - \frac{\tau_b}{\tau_{cd}}\right) \tag{32}$$

where $m(b)$ is particle concentration evaluated at the sea bottom, τ_b is bottom stress due to tides and the residual current, and τ_{cd} is a critical

deposition stress above which no deposition occurs since particles are maintained in suspension by water turbulence.

The settling velocity is determined from Stokes's law:

$$w_s = \frac{\rho - \rho_w}{\rho_w} \frac{gD^2}{18\nu} \quad (33)$$

where ρ and D are suspended particle density and diameter respectively and ν is kinematic viscosity of water. The erosion rate is written in terms of the erodability constant:

$$ER = Ef\left(\frac{\tau_b}{\tau_{ce}} - 1\right) \quad (34)$$

where E is the erodability constant, f gives the fraction of fine particles in the bed sediment and τ_{ce} is a critical erosion stress below which no erosion occurs. The model can also calculate sedimentation rates (SR) as the balance between the deposition and erosion terms.

References

Achterberg EP, Braungardt C, Morley NH, Elbaz-Poulichet F, Leblanc M. Impact of Los Frailes mine spill on riverine, estuarine and coastal waters in southern Spain. Water Res 1999;33:3387–94.

Ambar I, Howe MR. Observations of the Mediterranean outflow. 2, the deep circulation in the vicinity of the Gulf of Cadiz. Deep-Sea Res 1979;26A:555–68.

Batteen ML, Martinez JR, Bryan DW, Buch EJ. A modelling study of the coastal eastern boundary current system off Iberia and Morocco. J Geophys Res 2000;105 (C6):14173–95.

Beckers JM, Achterberg EP, Braungardt Ch. Comparison of high spatial resolution trace metal distributions with model simulations for surface waters of the Gulf of Cadiz. Estuar Coast Shelf Sci 2007;74:599–609.

Cancino L, Neves R. Hydrodynamic and sediment suspension modelling in estuarine systems. Part I: description of the numerical models. J Mar Syst, 1999;22:105–16.

Cetina M, Rajar R, Povinec P. Modelling of circulation and dispersion of radioactive pollutants in the Japan Sea. Oceanol Acta 2000;23:819–36.

Chen K, Jiao JJ. Metal concentrations and mobility in marine sediment and groundwater in coastal reclamation areas: a case study in Shenzhen, China. Environ Pollut 2008;151:576–84.

Cobelo-García A, Prego R, De Castro M. Metal distributions and their fluxes at the coastal boundary of a semi-enclosed ria. Mar Chem 2005;97:277–92.

Cravo A, Madureira M, Felicia H, Rita F, Bebianno MJ. Impact of outflow from the Guadiana River on the distribution of suspended particulate matter and nutrients in the adjacent coastal zone. Estuar Coast Shelf Sci 2006;70:63–75.

Criado-Aldeanueva F, García-Lafuente J, Vargas JM, del Río J, Vázquez A, Reul A, et al. Distribution and circulation of water masses in the Gulf of Cadiz from in situ observations. Deep-Sea Res II 2006;53:1144–60.

Cuong DT, Karuppiah S, Obbard JP. Distribution of heavy metals in the dissolved and suspended phase of the sea-surface microlayer, seawater column and in sediments of Singapore's coastal environment. Environ Model Assess 2008;138:255–72.

Dick S, Schonfeld W. Water transport and mixing in the North Frisian Wadden Sea. Results of numerical investigations. Ger J Hydrogr 1996;48:27–48.

Duursma EK, Carroll J. Environmental compartments. Berlin: Springer; 1996.

Dyke PPG. Coastal and Shelf Sea modelling. The Netherlands: Kluwer; 2001.

Eisma D. Suspended matter in the aquatic environment. Berlin: Springer-Verlag; 1993.

Elbaz-Poulichet F, Morley NH, Beckers JM, Nomerange P. Metal fluxes through the Strait of Gibraltar: the influence of the Odiel and Tinto Rivers (SW Spain). Mar Chem 2001;73:193–213.

Fabres J, Calafat A, Sanchez-Vidal A, Canals M, Heussner S. Composition and spatio-temporal variability of particle fluxes in the western Alborán gyre, Mediterranean Sea. J Mar Syst 2002;33/34:431–56.

Fernández-Caliani JC, Ruiz-Muñoz F, Galán E. Clay mineral and heavy metal distributions in the lower estuary of Huelva and adjacent Atlantic shelf, SW Spain. Sci Total Environ 1997;198:181–200.

Freitas PS, Abrantes F. Suspended particulate matter in the Mediterranean water at the Gulf of Cadiz and off the southwest coast of the Iberian Peninsula. Deep-Sea Res II 2002;49:4245–61.

García-Lafuente J, Ruíz J. The Gulf of Cadiz pelagic ecosystem: a review. Prog Oceanogr 2007;74:228–51.

García-Lafuente J, Delgado J, Criado-Aldeanueva F, Bruno M, del Río J, Vargas JM. Water mass circulation on the continental shelf of the Gulf of Cadiz. Deep-Sea Res II 2006;53:1182–97.

Gascó C, Antón MP, Delfanti R, González AM, Meral J, Pappuci C. Variation of the activity concentrations and fluxes of natural (^{210}Po, ^{210}Pb) and anthropogenic (^{239,240}Pu, ^{137}Cs) radionuclides in the Strait of Gibraltar (Spain). J Environ Radioact 2002;62:241–62.

Gómez F. The role of the exchanges through the Strait of Gibraltar on the budget of elements in the western Mediterranean Sea: consequences of human-induced modifications. Mar Pollut Bull 2003;46:685–94.

Gómez-Parra A, Forta JM, Delvalls TA, Sáenz I, Riba I. Early contamination by heavy metals of the Guadalquivir estuary after the Aznalcollar Mining Spill (SW Spain). Mar Pollut Bull 2000;40:1115–23.

Gonzalez R, Araujo MF, Burdloff D, Cachao M, Cascalho J, Corredeira C, et al. Sediment and pollutant transport in the northern Gulf of Cadiz: a multi-proxy approach. J Mar Syst 2007;68:1-23.

Harms IH. Modelling the dispersion of ^{137}Cs and ^{239}Pu released from dumped waste in the Kara Sea. J Mar Syst 1997;13:1-19.

Hernández-Molina FJ, Llave E, Stow DAW, García M, Somoza L, Vázquez JT, et al. The contourite depositional system of the Gulf of Cadiz: a sedimentary model related to the bottom current activity of the Mediterranean outflow water and its interaction with the continental margin. Deep-Sea Res II 2006;53:1420–63.

IAEA. Sediment distribution coefficients and concentration factors for biota in the marine environment. Technical Reports Series 2004;422 (Vienna).

Jensen TG. Open boundary conditions in stratified ocean models. J Mar Syst 1998;16:297–322.

Johnson J, Stevens I. A fine resolution model of the eastern North Atlantic between the Azores, the Canary Islands and the Gibraltar Strait. Deep-Sea Res I 2000;47:875–99.

Johnson J, Ambar I, Serra N, Stevens I. Comparative studies of the spreading of Mediterranean water through the Gulf of Cadiz. Deep-Sea Res II 2002;49:4179–93.

Jungclaus JH, Mellor GL. A three-dimensional model study of the Mediterranean outflow. J Mar Syst 2000;24:41–66.

Kowalick Z, Murty TS. Numerical modelling of ocean dynamics. Singapore: World Scientific; 1993.

Li Q, Wub Z, Chua B, Zhanga N, Caia S, Fanga J. Heavy metals in coastal wetland sediments of the Pearl River Estuary, China. Environ Pollut 2007;149:158–64.

Liu YP, Millward GE, Harris JRW. Modelling the distributions of dissolved Zn and Ni in the Tamar Estuary using hydrodynamics coupled with chemical kinetics. Estuar Coast Shelf Sci 1998;47:535–46.

Liu WC, Hsu MH, Kuo AY. Modelling of hydrodynamics and cohesive sediment transport in Tanshui River estuarine system, Taiwan. Mar Pollut Bull, 2002a;44:1076–88.

Liu JT, Chao S, Hsu RT. Numerical modeling study of sediment dispersal by a river plume. Cont Shelf Res 2002b;22:1745–73.

Lobo FJ, Sánchez R, González R, Dias JMA, Hernández-Molina FJ, Fernández-Salas LM, et al. Contrasting styles of the Holocene highstand sedimentation and sediment dispersal systems in the northern shelf of the Gulf of Cadiz. Cont Shelf Res 2004;24:461–82.

Lumborg U, Windelin A. Hydrography and cohesive sediment modelling: application to the Romo Dyb tidal area. J Mar Syst, 2003;38:287–303.

Machado A, Rocha F, Gomes C, Dias J. Distribution and composition of suspended particulate matter in Guadiana estuary (southwestern Iberian Peninsula). J Coast Res 2007;50:1040–5.

Machín F, Pelegrí JL, Marrero-Díaz A, Laiz I, Ratsimandresey AW. Near-surface circulation in the southern Gulf of Cadiz. Deep-Sea Res II 2006;53:1161–81.

Marín-Guirao L, Lloret J, Marin A. Carbon and nitrogen stable isotopes and metal concentration in food webs from a mining-impacted coastal lagoon. Sci Total Environ 2008;393:118–30.

Monte L, Hakason L, Periáñez R, Laptev G, Zheleznyak M, Maderich V, et al. Experiences from a case study of multi-model application to assess the behaviour of pollutants in the Dnieper–Bug estuary. Ecol Model 2006;195:247–63.

Morillo J, Usero J, Gracia I. Heavy metal distribution in marine sediments from the southwest coast of Spain. Chemosphere 2004;55:431–42.

Nyffeler UP, Li YH, Santschi PH. A kinetic approach to describe trace element distribution between particles and solution in natural aquatic systems. Geochim Cosmochim Acta 1984;48:1513–22.

NOAA. Computer Applications to Tides in the National Ocean Survey. Supplement to Manual of Harmonic Analysis and Prediction of Tides (Special Publication No. 98). National Ocean Service, National Oceanic and Atmospheric Administration. U.S. Department of Commerce; 1982. January 1982.

Palanques A, Plana F, Maldonado A. Estudio de la materia en suspensión en el Golfo de Cádiz. Acta Geol Hisp 1986–1987;21–22:491–7 (in Spanish).

Peliz A, Dubert J, Marchesielo P, Teles-Machado A. Surface circulation in the Gulf of Cadiz: model and mean flow structure. J Geophys Res 2007;112:C11015 (20 pages).

Periáñez R. Three dimensional modelling of the tidal dispersion of non conservative radionuclides in the marine environment. Application to ^{239,240}Pu dispersion in the eastern Irish Sea. J Mar Syst 1999;22:37–51.

Periáñez R. Modelling the tidal dispersion of ^{137}Cs and ^{239,240}Pu in the English Channel. J Environ Radioact 2000;49:259–77.

Periáñez R. The enhancement of ^{226}Ra in a tidal estuary due to the operation of fertilizer factories and redissolution from sediments: experimental results and a modelling study. Estuar Coast Shelf Sci 2002;54:809–19.

Periáñez R. Kinetic modelling of the dispersion of plutonium in the eastern Irish Sea: two approaches. J Mar Syst 2003;38:259–75.

Periáñez R. On the sensitivity of a marine dispersion model to parameters describing the transfers of radionuclides between the liquid and solid phases. J Environ Radioact 2004;73:101–15.

Periáñez R. Modelling the dispersion of radionuclides in the marine environment. Heidelberg: Springer-Verlag; 2005a.

Periáñez R. Modelling the transport of suspended particulate matter by the Rhone River plume (France). Implications for pollutant dispersion. Environ Pollut 2005b;133:351–64.

Periáñez R. A modelling study on ^{137}Cs and ^{239,240}Pu behaviour in the Alborán Sea, western Mediterranean. J Environ Radioact 2008;99:694–715.

Periáñez R, Pascual-Granged A. Modelling surface radioactive, chemical and oil spills in the Strait of Gibraltar. Comput Geosci 2008;34:163–80.

Periáñez R, Abril JM, García-León M. Modelling the suspended matter distribution in an estuarine system: application to the Odiel river in southwest Spain. Ecol Model 1996;87:169–79.

Periáñez R, Absi A, Villa M, Moreno HP, Manjón G. Self-cleaning in an estuarine area formerly affected by ^{226}Ra anthropogenic enhancements: numerical simulations. Sci Total Environ 2005;339:207–18.

Prandle D, Ballard G, Flatt D, Harrison J, Jones SE, Knight PJ, et al. Combining modelling and monitoring to determine fluxes of water, dissolved and particulate metals trough the Dover Strait. Cont Shelf Res 1996;16:237–57.
Pugh DT. Tides, surges and mean sea level. Chichester: Wiley; 1987.
Riba I, Del Valls TA, Forja JM, Gómez-Parra A. Influence of the Aznalcóllar minning spill on the vertical distribution of heavy metals in sediments from the Guadalquivir estuary (SW Spain). Mar Pollut Bull 2002;44:39–47.
Sainz A, Ruiz F. Influence of the very polluted inputs of the Tinto–Odiel system on the adjacent littoral sediments of southwestern Spain: a statistical approach. Chemosphere 2006;62:1612–22.
Schwiderski EW. Ocean tides, part 1: global ocean tidal equations. Mar Geod 1980a;3:161–217.
Schwiderski EW. Ocean tides, part 2: a hydrodynamical interpolation model. Mar Geod 1980b;3:219–55.
Scott EM. Modelling radioactivity in the environment. UK: Elsevier; 2003.
Serra N, Ambar I, Kase RH. Observations and numerical modelling of the Mediterranean outflow splitting and eddy generation. Deep-Sea Res II 2005;52:383–408.
Suntornvongsagula K, Burkeb DJ, Hamerlynckb EP, Hahna D. Fate and effects of heavy metals in salt marsh sediments. Environ Pollut 2007;149:79–91.
Tappin A, Burton JD, Millward GE, Statham PJ. A numerical transport model for predicting the distributions of Cd, Cu, Ni, Pb and Zn in the southern North Sea: the sensitivity of model results to the uncertainties in the magnitudes of metal inputs. J Mar Syst 1997;13:173–204.
Tattersall GR, Elliott AJ, Lynn NM. Suspended sediment concentrations in the Tamar estuary. Estuar Coast Shelf Sci 2003;57:679–88.
Tejedor L, Izquierdo A, Kagan BA, Sein DV. Simulation of the semidiurnal tides in the Strait of Gibraltar. J Geophys Res 1999;104:13541–57.
Tsimplis MN, Proctor R, Flather RA. A two dimensional tidal model for the Mediterranean Sea. J Geophys Res 1995;100:16223–39.
Valdés J, Romám D, Alvarez G, Ortlieb l, Guiñez M. Metals content in surface waters of an upwelling system of the northern Humboldt Current (Mejillones Bay, Chile). J Mar Syst 2008;71:18–30.
Vested HJ, Baretta JW, Ekebjærg LC, Labrosse A. Coupling of hydrodynamical transport and ecological models for 2D horizontal flow. J Mar Syst 1996;8:255–67.
Wen LS, Santschi P, Gill G, Paternostro C. Estuarine trace metal distributions in Galvelstone Bay: importance of colloidal forms in the speciation of the dissolved phase. Mar Chem 1999;63:185–212.
Wolanski E, Chicharo L, Chicharo MA, Morais P. An ecohydrology model of the Guadiana estuary (South Portugal). Estuar Coast Shelf Sci 2006;70:132–43.
Wu Y, Falconer R, Lin B. Modelling trace metal concentration distributions in estuarine waters. Estuar Coast Shelf Sci 2005;64:699–709.
Yanagi T. Coastal oceanography. The Netherlands: Kluwer; 1999.